# Computationally Efficient Blind Equalization

D.R. Brown, P.B. Schniter, and C.R. Johnson, Jr.*

**Abstract:** Adaptive blind equalization has gained wide-spread use in communication receivers that operate without training signals. In particular, the Constant Modulus Algorithm (CMA) [6, 10] has become a favorite of practitioners due to its LMS-like complexity and desirable robustness properties [4, 5, 14]. This paper presents a signed-error version of CMA (SE-CMA) which is motivated by a further reduction in the computation complexity of the equalizer coefficient update. The authors investigate the performance of SE-CMA and establish connections to previously proposed signed blind algorithms. A novel dithered signed blind algorithm (DSE-CMA) is proposed which overcomes significant SE-CMA convergence issues and possesses similar robustness properties to the standard (i.e. unsigned) CMA.

## 1 Introduction

Digital communication through band-limited or multipath channels results in inter-symbol interference (ISI) which, if left uncompensated, can cause unnecessarily high symbol error rates (SER) at the receiver. One popular approach to the mitigation of ISI, termed linear equalization, employs a linear transversal filter at the receiver input. The optimal equalizer achieves the performance goal of minimum SER, however, since SER is a highly nonlinear function of the filter coefficients [13], the minimum-mean-squared-error (MMSE) criterion is commonly used as a close proxy. The least-mean-squares (LMS) algorithm gives a practical adaptive solution to finding the MMSE equalizer when the receiver shares knowledge of a training sequence. Particular circumstances, such as time-varying channels, may force frequent re-transmission of the training sequence, leading to inefficient use of available bandwidth. These drawbacks motivate schemes for *blind* adaptive equalization, where only the statistics of the transmitted signal need be known.

Several Bussgang [2] blind equalization schemes have been proposed over the last 20 years, including those that minimize the Benveniste-Goursat-Ruget [1] and Godard [6] (or constant modulus [10]) criteria. Over the last decade, the Constant Modulus Algorithm (CMA) has established itself as the most popular method for the blind adaptation of linear equalizers. The primary reasons for CMA's success lie in its LMS-like complexity and robustness to the factors present in a typical implementation scenario: additive channel noise, lack of channel disparity, and "short" equalizer lengths. Furthermore, it has been shown that under "ideal" operating conditions, CMA achieves perfect symbol recovery, thus performing as well as any non-blind equalization algorithm.

Though noted for its computational efficiency, CMA may be further simplified by transforming the bulk of its multiplications during the equalizer update into sign operations. The reductions in implementation cost have the potential of making feasible the application of blind equalization to low-cost communication products.

*Authors with Cornell University, Ithaca, NY 14853. Supported in part by NSF grant MIP-9509011 and Applied Signal Technology.

Signed versions of the LMS algorithm leave behind a valuable body of literature (see for example [3, 11]). Immediately evident from this literature (and from routine simulations) is that the signed algorithm behaves quite differently than the original algorithm under normal circumstances. Hence, the application of typical signed-update strategies to CMA may undermine the robustness which motivates its use in the first place.

This paper shows that although SE-CMA performs well in the "ideal" case, the robustness properties of CMA are compromised in a realistic environment. As a solution to the observed defect, we present a novel version of SE-CMA which preserves much of the behavior of the original CMA. It evolves from the consideration of the sign operation as a one-bit quantization and employs a dither signal made suitable by the averaging inherent to the stochastic gradient descent (SGD) update.

## 1.1 System Model

In this paper, we restrict our focus to the case of a noiseless communication system with a FIR channel model and a fractionally-spaced equalizer (FSE) [9] with sampling interval $T/2$ (where $T$ is the symbol period). The source symbols are chosen from a finite, zero-mean alphabet. The system may be represented by the multirate model in Figure 1, where $s_n$ is the baud-spaced source symbol at sample index $n$, $\mathbf{c}$ is the the vector representing the fractionally-spaced channel impulse response, $\mathbf{f}$ is the vector containing the fractionally-spaced equalizer coefficients, and $y_n$ is the baud-spaced equalizer output. The number of coefficients in the channel and equalizer response vectors are $N_c$ and $N_f$, respectively. The system output may be expressed as $y_n = \mathbf{s}^t(n)\,\mathbf{C}\,\mathbf{f}$ where $\mathbf{s}(n) = [s_n, s_{n-1}, \ldots, s_{n-N_s+1}]^t$ is the length-$N_s = \lfloor (N_c + N_f - 1)/2 \rfloor$ vector of baud-spaced source symbols and $\mathbf{C}$ is the $N_s \times N_f$ decimated channel convolution matrix given by

$$\mathbf{C} = \begin{bmatrix} c_1 & c_0 & & & & & \\ \vdots & \vdots & c_1 & c_0 & & & \\ c_{N_c-1} & c_{N_c-2} & \vdots & \vdots & \ddots & c_1 & c_0 \\ & & c_{N_c-1} & c_{N_c-2} & \ddots & \vdots & \vdots \\ & & & & & c_{N_c-1} & c_{N_c-2} \end{bmatrix}.$$

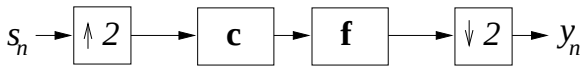


Figure 1: Noiseless $T/2$-spaced multirate system model.

## 1.2 The Constant Modulus Algorithm

The constant modulus (CM) criterion may be expressed by the non-negative cost function $J_{cma_{p,q}}$ parameterized by positive integers $p$ and $q$:

$$J_{cma_{p,q}} = \frac{1}{pq} E\left\{ \left| |y_n|^p - \gamma \right|^q \right\}, \tag{1}$$

where $\gamma$ is a fixed constant[1] [6, 10]. Two key observations are

[1]The CM criterion is most often implemented as CMA 2-2 ($p, q = 2$) and in this case $\gamma = E\{|s_n|^4\}/E\{|s_n|^2\}$. We hereapon assume these values unless noted otherwise.

- The CM cost function is insensitive to phase variations in the received signal. This is useful in receiver designs that attempt to separate carrier synchronization from equalization (e.g. allowing a higher performance carrier recovery loop).
- The CM criterion penalizes the dispersion of received signal modulus, $E\{|y_n|^p\}$, about $\gamma$. As a phase-independent criterion for blind source recovery, minimizing dispersion seems intuitively satisfying for CM sources (e.g. $M$-PSK). Remarkably, the CM criterion also works well with non-CM sources (e.g. $M$-PAM and $M$-QAM).

Adaptive implementation using SGD leads to the CMA equalizer update equation:

$$\mathbf{f}(n+1) \;=\; \mathbf{f}(n) + \mu \mathbf{r}^*(n)\psi(y_n), \tag{2}$$

where $\mathbf{f}$ is the length-$N_f$ equalizer coefficient vector, $\mathbf{r}(n)$ is the length-$N_f$ receiver input vector (i.e. regressor), $\mu$ is a (small) step-size, and

$$\psi(y_n) \;=\; -\nabla_{y_n} \frac{1}{4}\left(|y_n|^2 - \gamma\right)^2 \;=\; y_n\left(\gamma - |y_n|^2\right) \tag{3}$$

is the CM error function.

It has been shown in [12] that, under ideal conditions, equalizers minimizing the CM cost function perfectly recover the original source symbols, i.e. $y_n = s_{n-\delta}$ for some system delay $\delta$. These perfect blind equalization (PBE) conditions [9] are stated below. Conditions **(A1)** though **(A3)** are required for the possibility of perfect symbol recovery (PSR), whereas conditions **(A4)** and **(A5)** are required to blindly achieve PSR.

**(A1)** Sufficient equalizer length: For an even-length channel and a $T/2$-spaced FSE, a necessary condition for channel invertibility is that $N_f \geq N_c - 2$.

**(A2)** Subchannel disparity: For the even-length $T/2$-spaced channel impulse response $\mathbf{c} = [c_0, c_1, \ldots, c_{N_c-1}]$, consider the polynomials formed by the even and odd coefficients of $\mathbf{c}$, i.e. $c_e(z^{-1}) = c_0 + c_2 z^{-1} + \cdots + c_{N_c-2} z^{-\frac{N_c}{2}+1}$ and $c_o(z^{-1}) = c_1 + c_3 z^{-1} + \cdots + c_{N_c-1} z^{-\frac{N_c}{2}+1}$. A necessary condition for perfect channel invertibility is that $c_e(z^{-1})$ and $c_o(z^{-1})$ have no common roots.

**(A3)** No additive channel noise.

**(A4)** Sub-Gaussian source: The source kurtosis $\kappa = \frac{E\{|s_n|^4\}}{E\{|s_n|^2\}^2}$ must satisfy $\kappa < 3$ for a real-valued source or $\kappa < 2$ for a complex-valued source.

**(A5)** White source: The source symbols must be temporally uncorrelated.

An attractive feature of CM equalizers is their robustness to violations of the PBE conditions. For example, CM equalizers have been shown to be quite robust to under-modelling [4], additive channel noise [5, 14], and lack of channel disparity [5].

# 2 SE-CMA for a Real-Valued Source

Typically, a signed-error algorithm modifies the equalizer update equation of the unsigned algorithm by retaining only the sign of the error function. The attractiveness of this modification is that, when $\mu$ is implemented as a fixed bit shift, the $N_f$ regressor multiplies

in (2) can be eliminated. Using the standard definition of the sign function for a real-valued argument, (2) can be modified to yield the SE-CMA equalizer update equation

$$\mathbf{f}(n+1) \;=\; \mathbf{f}(n) + \mu \mathbf{r}(n) \underbrace{\operatorname{sgn}\big(\psi(y_n)\big)}_{\triangleq \sigma(y_n)}. \tag{4}$$

The CMA and SE-CMA error functions are compared in Figure 2.

The SE-CMA error function (like CMA) satisfies the Benveniste-Goursat-Ruget Theorem [1] which requires that the function $g(y) = y + \sigma(y)$ satisfies $g(0^+) \geq 0$ and $g''(y) \leq 0$ for $y > 0$, where at least one of the two inequalities must be strict. Since $\sigma(0^+) = 1$ and $\sigma''(y) = 0$ for $y > 0$, we conclude from the BGR Theorem that, under the PBE conditions, SE-CMA converges to an equalizer solution providing perfect symbol recovery.

## 2.1 Relationships to Other Blind Equalization Algorithms

Consider the CMA 1-1 cost function $J_{cma_{1,1}} = E\big\{\big||y_n| - \beta\big|\big\}$. The corresponding SGD algorithm is obtained by taking the instantaneous gradient of $J_{cma_{1,1}}$, given by

$$\begin{aligned} \nabla_{y_n}\big||y_n| - \beta\big| &= \operatorname{sgn}(\beta - |y_n|)\operatorname{sgn}(y_n) \\ &= \operatorname{sgn}\big(y_n(\beta - |y_n|)\big) \end{aligned}$$

for $y \notin \{-\beta, 0, \beta\}$. The CMA 1-1 update then becomes $\mathbf{f}(n+1) = \mathbf{f}(n) + \mu \mathbf{r}(n) \operatorname{sgn}(y_n(\beta - |y_n|))$ which is equivalent to SE-CMA when $\beta = \sqrt{\gamma}$.

Now consider the signed-Sato algorithm [15] (for real-valued observations): $\mathbf{f}(n+1) = \mathbf{f}(n) + \mu \mathbf{r}(n) \operatorname{sgn}(\rho \operatorname{sgn}(y_n) - y_n)$. Using straightforward algebra, it can be shown that the signed-Sato algorithm is equivalent to SE-CMA when $\rho = \sqrt{\gamma}$.

It is also straightforward to show that the Signed Godard Algorithm proposed by Weerackody (WSGA) in [16] with real valued observations is equivalent to SE-CMA.

Thus *SE-CMA* $\Leftrightarrow$ *signed-Sato* $\Leftrightarrow$ *CMA 1-1* $\Leftrightarrow$ *SGA* for real-valued communication systems. The following examples and analyses apply to each of these algorithms.

## 2.2 Properties of the Noiseless SE-CMA Cost Surface

We denote the set of points in the domain of the SE-CMA error function $\sigma(\cdot)$ leading to discontinuity as $\mathcal{D} = \{-\sqrt{\gamma}, 0, \sqrt{\gamma}\}$. Assuming that the source symbols are selected from a finite $M$-ary alphabet, the source vector $\mathbf{s}$ will have $M^{N_s}$ possible realizations. We denote this set of all possible $\mathbf{s}$ by $\mathcal{S}$. Using a similar approach as in [3], note that the sizes of $\mathcal{D}$ and $\mathcal{S}$ imply that there are $3M^{N_s}$ hyperplanes of dimension $N_f - 1$ in the equalizer parameter space containing $\mathbf{f}$ that satisfy

$$y = \mathbf{s}^t \mathbf{C} \mathbf{f}, \;\text{ for } \mathbf{s} \in \mathcal{S} \text{ and } y \in \mathcal{D}. \tag{5}$$

These equalizer-space hyperplanes define boundaries across which the sign of the SE-CMA error function changes. In other words, within any convex region $\mathcal{R} \in \mathbb{R}^{N_f}$ *not* subdivided by any sign boundary, the SE-CMA error function remains constant.

For adequately small step-sizes and equiprobable $\mathbf{s} \in \mathcal{S}$, the expected trajectory step for any equalizers within the interior of a given region $\mathcal{R}$ is

$$E\{\mathbf{f}(n+1) - \mathbf{f}(n)\} = \mu M^{-N_s} \sum_{\mathbf{s} \in \mathcal{S}} \mathbf{s}^t \mathbf{C}\, \sigma(\mathbf{s}^t \mathbf{C} \mathbf{f}_{\mathcal{R}}) \tag{6}$$

where $\mathbf{f}_{\mathcal{R}}$ is any equalizer in $\mathcal{R}$. Observe that there is only one average trajectory associated with each region $\mathcal{R}$.

## 2.3 Illustrative Examples

In this section, we illustrate several important properties of SE-CMA using examples constructed with two-tap equalizers. This permits visualization of the cost surface in equalizer-coefficient space. Conveniently, the sign-boundary hyperplanes become lines and the regions $\mathcal{R}$ created by these lines are 2-dimensional tiles in the equalizer plane. Furthermore, the fact that the average trajectory update is constant within a tile implies that the two-tap SE-CMA (or CMA 1-1) cost surface is composed of flat facets.

### 2.3.1 Perfect Blind Equalization with BPSK source

Consider the communication system in Figure 1 with an i.i.d. BPSK source, the noiseless channel $\mathbf{c}_a = [0.2, 0.5, 1, -0.1]^t$, and a two-tap FSE. Here, the set $\mathcal{S}$ is composed of the columns of $\mathbf{S} = \left[\begin{smallmatrix} -1 & -1 & 1 & 1 \\ -1 & 1 & -1 & 1 \end{smallmatrix}\right]$ and the channel convolution matrix is $\mathbf{C} = \left[\begin{smallmatrix} 0.5 & 0.2 \\ -0.1 & 1 \end{smallmatrix}\right]$. Figure 3 shows the sign-boundaries from (5) overlaid on the CMA 2-2 cost surface contours in equalizer space and several SE-CMA equalizer trajectories. Note the following:

- Within the interior of a given facet, the SE-CMA trajectories tend to follow a linear path in the direction of steepest descent.
- The trajectories closely follow boundaries between two facets whose gradients both point in the direction of the boundary. Looking closely, the trajectories actually "bounce" between such facet pairs.
- The trajectories converge to the intersection of four facets whose gradients all point in the direction of the intersection. These stable intersections coincide with the stable stationary points of the CMA 2-2 cost surface, which in the PBE case correspond to perfect symbol recovery. Given the BGR Theorem, this global convergence is expected. Note that the unstable intersections coincide with the unstable stationary points of the CMA 2-2 cost surface (in this case, 4 saddle points and one maximum).

### 2.3.2 Perfect Blind Equalization with 8-PAM source

Now consider the same communication system except with source symbols chosen from a unit-variance 8-PAM alphabet. The increase in the size of the source alphabet leads to an exponential increase in the number of sign-boundaries. For a two-tap equalizer, they are plotted in Figure 4.

Notice that the 8-PAM SE-CMA cost surface is considerably more complicated due to the large number of facets. In general, neighboring facets do not necessarily have opposing gradients and thus equalizer trajectories may cross sign boundaries and assume a new average trajectory toward the perfect equalization solution. Also notice that the stable intersections of sign-boundaries do *not* coincide with the PSR minima as expected from the BGR Theorem but instead appear to be collinear with the PSR minima. This is due to the fact that the choice of $\gamma = E\{s^4\}/E\{s^2\}$ as specified by CMA 2-2 is not appropriate for SE-CMA with non-CM sources such as BPSK. However, as the BGR Theorem predicts, there is a value for $\gamma$ for which SE-CMA converges to the perfect equalizer. Specifically, $\gamma$ should be chosen such that $\gamma = a_\nu^2$ where $a_\nu$ is the $\nu^{th}$ positive member of the source alphabet and integer $\nu$ satisfies

$$\nu = \arg\min_k \frac{\left(k - \frac{1}{2}\left(1 + \sqrt{\frac{M^2}{2} - 1}\right)\right)^2}{k - \frac{1}{2}}. \tag{7}$$

The proof is provided in Appendix A. For the 8-PAM unit-variance alphabet, (7) suggests $\gamma = 25/21$. Figure 5 shows that perfect equalization is achieved for this value of $\gamma$.

### 2.3.3 Undermodelled channel with BPSK source

The question remains, "How well does SE-CMA work under a practical context?" The following examples illustrate the behavior of SE-CMA in more realistic conditions by violating PBE condition **(A1)**, otherwise known as channel undermodelling. This situation nearly always occurs in practice. Consider the communication system in Section 2.3.1 but with channel $\mathbf{c}_b = [0.1, 0.3, 1, -0.1, 0.5, 0.2]^t$. Figure 6 shows the CMA 2-2 cost surface contours and the SE-CMA sign-boundaries with $\mathcal{S}$ composed of the columns of $\mathbf{S} = \begin{bmatrix} -1 & -1 & -1 & -1 & 1 & 1 & 1 & 1 \\ -1 & -1 & 1 & 1 & -1 & -1 & 1 & 1 \\ -1 & 1 & -1 & 1 & -1 & 1 & -1 & 1 \end{bmatrix}$ and the channel convolution matrix is $\mathbf{C} = \begin{bmatrix} 0.3 & 0.1 \\ -0.1 & 1 \\ 0.2 & 0.5 \end{bmatrix}$.

Examine the two SE-CMA trajectories in Figure 6. The trajectory labeled $A$ converges to a stable intersection point of the sign-boundaries in the neighborhood of (but not collinear with) the CMA 2-2 and MMSE minima. Trajectory $B$, on the other hand, does not converge to any point on the cost surface after 10000 iterations. This failure to converge can be explained by calculating the average trajectory in this tile using (6), from which we obtain the alarming result that $E\{\mathbf{f}(n+1) - \mathbf{f}(n)\} = 0$. Although the instantaneous trajectory will be non-zero, the zero-valued average update has the potential of capturing the trajectory for an arbitrarily long time.

Simulations suggest that *zero-slope facets* always exist for both BPSK and $M$-PAM sources in the case of channel undermodelling. This seriously undermines the applicability of SE-CMA to practical communication systems in high-SNR environments. As an alternative, we propose a novel signed-update algorithm that retains the computational efficiency of SE-CMA while exhibiting the desirable robustness properties of CMA 2-2. As such, it is unhindered by the existence of zero-slope facets.

# 3 Dithered SE-CMA

*"Gimme noise, noise, noise, noise ... "* —*Paul Westerberg,* Stink, *1982.*

This section describes a simple modification to SE-CMA that results in an algorithm which, for small step-sizes, behaves remarkably like the original CMA while retaining the computational efficiency of SE-CMA.

Viewing the sign operation in SE-CMA as a one-bit quantizer, it makes sense to consider the application of *dither* [7]. Dithering techniques attempt to preserve information lost in the quantization process by making the quantization noise white and independent of the signal being quantized. Such techniques[2] accomplish these properties by adding a random process (*dither*) to the information signal before quantization.

The dithered SE-CMA (DSE-CMA) algorithm is formed by dithering the SE-CMA error function with $d_n$:

$$\mathbf{f}(n+1) \;=\; \mathbf{f}(n) - \mu \mathbf{r}(n) \underbrace{\operatorname{sgn}\big(\psi(y_n) + d_n\big)}_{\triangleq \varphi(y_n)}. \tag{8}$$

In our case, a simple but useful $d_n$ is an i.i.d. sequence uniformly distributed on $(-1, 1]$. Using the theorems in [7], it can be shown that this dither has the desirable property

[2]See [8] for an application of dither to LMS-based echo cancellation.

that the quantization noise $\epsilon_n = \varphi(y_n) - \psi(y_n)$ is zero-mean and uncorrelated with $\psi(y_n)$ for $|\psi(y_n)| < 1$. In other words, the random function $\varphi$ is a "clipped" version of the CMA error function $\psi$:

$$E\{\varphi|y\} = \begin{cases} -1 & y : \psi(y) < -1, \\ 1 & y : \psi(y) > 1, \\ \psi & \text{else.} \end{cases} \tag{9}$$

For small $\mu$, the averaging inherent in DSE-CMA sufficiently approximates the expectation in 9. In this case, we can conclude that DSE-CMA should closely follow the average CMA 2-2 trajectories. Furthermore, the zero-mean property of the quantization noise leads us to believe that DSE-CMA should exhibit mean convergence to a (local) CMA solution. Figure 7 presents simulation results demonstrating these claims. Note that DSE-CMA trajectories appear to descend the CMA 2-2 error surface, not the faceted SE-CMA error surface. Unlike SE-CMA, the trajectories are not captured by zero-slope facets.

The principle disadvantage of DSE-CMA over CMA 2-2 is its higher *excess CM-cost*, defined as the increase in steady-state CM-cost over the (locally) minimum CM-cost [9]. A variable step-size, or "gearshift" algorithm could help remedy this undesired steady-state behavior without compromising convergence speed.

# 4 SE-CMA for a complex-valued source

As mentioned in Section 1.2, a key feature of CMA is that its convergence is unhindered by variations in the complex-valued received signal phase. We desire a computationally-efficient algorithm (i.e. no regressor multiplies) with the same property.

First, consider extending the real-valued $\mathrm{sgn}(\cdot)$ function in (4) to $\mathrm{csgn}(x) = \mathrm{sgn}(\mathrm{Re}\, x) + j\,\mathrm{sgn}(\mathrm{Im}\, x)$. Using straightforward algebra, we obtain the complex-valued SE-CMA update equation $\mathbf{f}(n+1) = \mathbf{f}(n) + \mu \mathbf{r}^*(n)\,\mathrm{csgn}(y_n)\,\mathrm{sgn}(\gamma - |y_n|^2)$, where $\gamma$ is a source dependent constant. We can compare this to a technique proposed by Weerackody in [16], termed the Signed Godard Algorithm (WSGA) and specified by the update $\mathbf{f}(n+1) = \mathbf{f}(n) + \mu \mathbf{r}^*(n)\,\mathrm{csgn}(y_n)\,\mathrm{sgn}(\beta - |\,\mathrm{Re}\, y_n| - |\,\mathrm{Im}\, y_n|)$. Note that WSGA attempts to force the equalized constellation onto a square rotated 45° in the complex plane, while SE-CMA attempts to force the constellation to a (constant-modulus) circle.

The phase-dependence of the WSGA "modulus-restoral" term, $\mathrm{sgn}(\beta - |\,\mathrm{Re}\, y_n| - |\,\mathrm{Im}\, y_n|)$, makes it susceptible to convergence problems when in the presence of carrier frequency offset. Intuitively, this carrier frequency offset can be considered a rapidly time-varying channel characteristic for which a small step-size algorithm like WSGA may be incapable of tracking. We note that this is not the case for the "modulus-restoral" term in SE-CMA: $\mathrm{sgn}(\gamma - |y_n|^2)$. However, we should not overlook the phase-dependent term $\mathrm{csgn}(y_n)$ present in both WSGA and SE-CMA.

The phase-independence of the CMA 2-2 update equation given by (2) and (3) is made possible by the interaction of the terms $\mathbf{r}^*(n)$ and $y_n$: they completely cancel the effects of received-signal phase-change on the equalizer update. In SE-CMA, however, the pair $\mathbf{r}^*(n)y_n$ is replaced by $\mathbf{r}^*(n)\,\mathrm{csgn}(y_n)$, which unfortunately does not retain this phase-independence property. Simulations have shown, however, that the "4-quadrant quantization" imposed by the $\mathrm{csgn}(\cdot)$ operation is sufficiently averaged by the recursive nature of SE-CMA, permitting fast convergence in the presence of large or small amounts of carrier-frequency offset.

# 5 Conclusion

This paper studies the SE-CMA real-valued equalization algorithm (and equivalents), derives the appropriate SE-CMA dispersion constant for $M$-PAM sources, and demonstrates significant convergence issues in the undermodelled, noiseless case. We propose a dithering technique that addresses this issue while retaining the computational efficiency of SE-CMA. Subsequent research focuses on two open problems: an understanding of the transient and asymptotic behavior of these algorithms in the presence of AWGN and the search for a computationally efficient complex-valued equalization algorithm retaining the phase-insensitivity of CMA.

# References


[1] A. Benveniste, et al., "Robust Identification of a Nonminimum Phase System: Blind Adjustment of a Linear Equalizer in Data Communications," *IEEE Trans. on Automatic Control*, vol. 25 no. 3, pp. 385-399, June 1980.

[2] S. Bellini, "Bussgang techniques for blind deconvolution and equalization," in *Blind Deconvolution*, Englewood Cliffs, NJ: Prentice-Hall, 1994, pp. 60-120.

[3] C. R. Elevitch et al., "Quiver Diagrams and Signed Adaptive Filters," *IEEE Trans. on Acoustics, Speech, and Signal Processing*, vol. 37, no. 2, pp. 227-235, Feb. 1989.

[4] T. J. Endres, et al., "On the Robustness of the Fractionally-Spaced Constant Modulus Criterion to Channel Order Undermodeling: Part I," in *Proc. IEEE Signal Processing Workshop on Signal Processing Advances in Wireless Communications* (Paris, France), pp. 37-40, 16-18 Apr. 1997.

[5] I. Fijalkow, et. al, "Fractionally spaced equalization using CMA: robustness to channel noise and lack of disparity," *IEEE Trans. on Signal Processing*, vol. 45, no. 1, pp. 56-66, Jan. 1997.

[6] D.N. Godard, "Self-Recovering Equalization and Carrier Tracking in Two-Dimensional Data Communication Systems," *IEEE Trans. on Communications*, vol. 28, no. 11, pp. 1867-1875, Nov. 1980.

[7] R.M. Gray et al., "Dithered Quantizers," *IEEE Trans. on Information Theory*, vol. 39, no. 3, pp. 805-812, May 1993.

[8] M. Bonnet and O. Macchi, "A low complexity echo canceller performing the channel phase acquisition," *IEEE Trans. on Acoustics, Speech, and Signal Processing*, vol. 34, no. 1, pp. 200-202, Feb. 1986.

[9] C.R. Johnson et al., "Blind Equalization Using the Constant Modulus Criterion: A Review," Submitted to *Proceedings of the IEEE*, Mar. 1997.

[10] J.R. Treichler et al., "A new approach to multipath correction of constant modulus signals," *IEEE Trans. on Acoustics, Speech, and Signal Processing*, vol. ASSP-31, no.2, pp. 459-72, Apr. 1983.

[11] W. A. Sethares, et al., "Adaptive Algorithms with Nonlinear Data and Error Functions," *IEEE Trans. on Signal Processing*, vol. 40, no. 9, pp. 2199-206, Sept. 1992.

[12] Ye Li et al., "Global convergence of fractionally-spaced Godard (CMA) adaptive equalizers," *IEEE Trans. on Signal Processing*, vol. 44, no.4, pp. 818-26, Apr. 1996.

[13] J.G. Proakis, *Digital Communications*, 3rd ed., New York, NY:McGraw-Hill, 1989.

[14] H.H. Zeng et al., "On the performance of CMA in the presence of noise," in *Proc. Conference on Information Science and Systems* (Princeton, NJ), pp. 890-894, Mar., 1996.

[15] V. Weerackody, et al., "A convergence model for the analysis of some blind equalization algorithms," in *Proc. IEEE International Symposium on Circuits and Systems* (), pp. 2136-2139, 1989.

[16] V. Weerackody, et al., "A simple hard-limited adaptive algorithm for blind equalization," *IEEE Trans. on Circuits and Systems*, vol. 39, no. 7, pp. 482-487, July 1992.

# A Selection of $\gamma$ for $M$-PAM sources

In this section we derive the unique positive $\gamma$ that provides perfect blind equalization for SE-CMA and an $M$-PAM source under the PBE conditions. The BGR Theorem tells us that such a $\gamma$ exists, and the equivalence between the SE-CMA solutions and the CMA 1-1 minima provides a straightforward method of finding this optimal $\gamma$.

We begin with the CMA 1-1 cost function $J(\gamma, \mathbf{h}) = E\left\{\left||\mathbf{s}^t\mathbf{h}| - \sqrt{\gamma}\right|\right\}$, written in terms of $\gamma$ and the system response $\mathbf{h} = \mathbf{Cf}$. Perfect symbol recovery requires that $\mathbf{h} = \mathbf{e}_\delta$, where $\mathbf{e}_\delta$ denotes a standard basis vector (i.e. $e_\delta = 1$ and $e_{i\neq\delta} = 0$). Before proceeding, we make two important observations: (i) the BGR Theorem implies that $J(\gamma_{opt}, \mathbf{h})$ is minimized by $\mathbf{h} = \mathbf{e}_\delta$, and (ii) the form of $J(\gamma, \mathbf{h})$ implies that changes in $\gamma$ scale the cost surface radially in $\mathbf{h}$-space. From these points we conclude that, for any $\gamma$, the CMA 1-1 minima are constrained to the set $\alpha\,\mathbf{e}_\delta$ (where $\alpha$ is a real scalar constant). This allows us to define the problem as follows:

$$\text{Find } \gamma \text{ such that } J(\gamma, \mathbf{e}_\delta) = \min_\alpha J(\gamma, \alpha\mathbf{e}_\delta). \tag{10}$$

For an $M$-PAM equiprobable source, $J(\gamma, \alpha\mathbf{e}_\delta) = \frac{2}{M}\sum_{l=1}^{M/2} |\alpha a_l - \sqrt{\gamma}|$, where $a_l$ denotes the $l^{th}$ positive alphabet member. Using straightforward algebra, it can be shown that the value of $\alpha$ minimizing this quantity is $\alpha_{min} = \sqrt{\gamma}/a_\nu$ for the integer $\nu$ satisfying

$$\nu = \arg\min_k \quad \sqrt{\gamma}\left(\frac{\left(\frac{M}{2}\right)^2 + 2k^2 - 1}{2k-1} - \left(\frac{M}{2}+1\right)\right) \tag{11}$$

Completing the square in (11) yields (7). Since $\nu$ may be determined without knowledge of $\gamma$, we can rewrite (10) as

$$\text{Find } \gamma \text{ such that } \frac{2}{M}\sum_{l=1}^{M/2} |a_l - \sqrt{\gamma}| = \frac{2}{M}\sum_{l=1}^{M/2}\left|\frac{\sqrt{\gamma}}{a_\nu}a_l - \sqrt{\gamma}\right|, \tag{12}$$

from which it is clear that $\gamma_{opt} = a_\nu^2$.

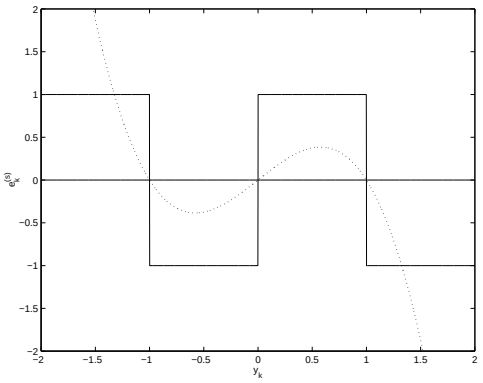

Figure 2: SE-CMA error function $\sigma(\cdot)$ (solid), and CMA error function $\psi(\cdot)$ (dotted), for $\gamma = 1$.

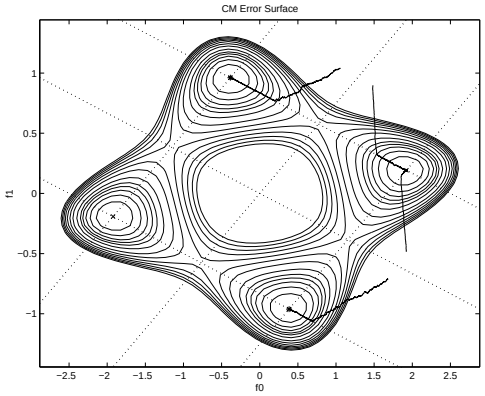


Figure 3: SE-CMA trajectories and sign-boundaries overlaid on CMA 2-2 cost contours for BPSK over channel $\mathbf{c}_a$.

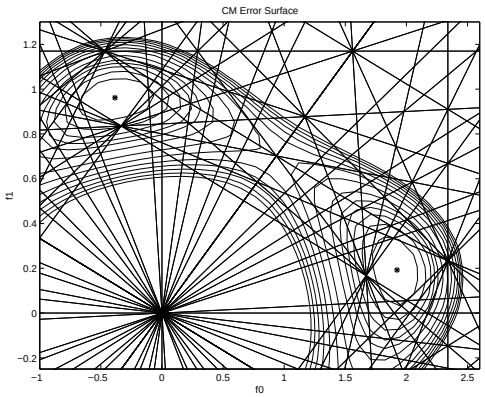


Figure 4: SE-CMA sign-boundaries for 8-PAM over noiseless channel $\mathbf{c}_a$ with $\gamma$ chosen as for CMA 2-2.

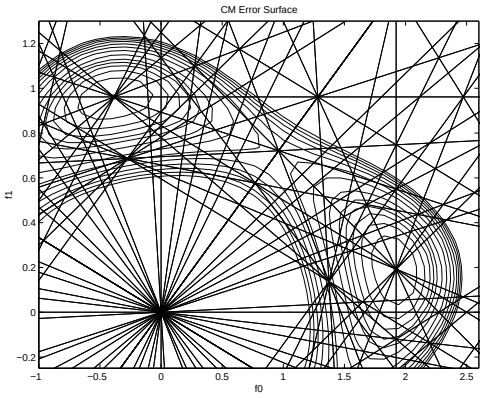


Figure 5: SE-CMA sign-boundaries for 8-PAM over noiseless channel $\mathbf{c}_a$ with $\gamma$ chosen via Section 2.3.2.

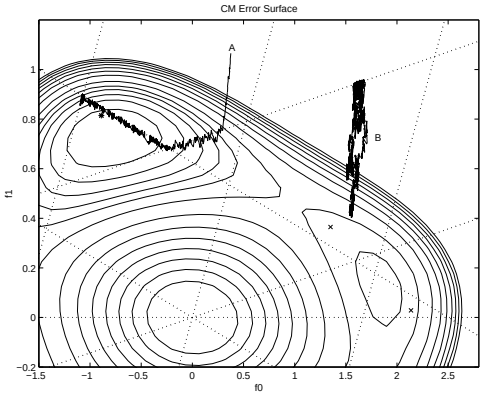


Figure 6: SE-CMA trajectories and sign-boundaries for BPSK over noiseless channel $\mathbf{c}_b$ with $\gamma = 1$.

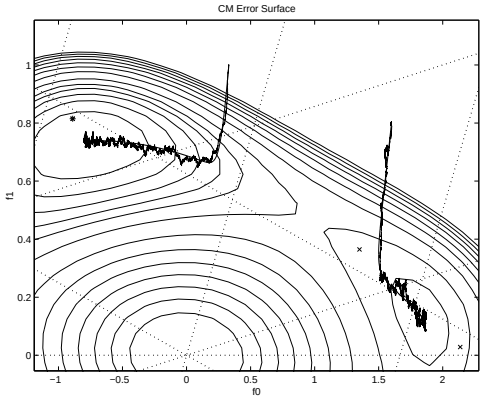


Figure 7: (Rough) DSE-CMA trajectories overlaid on (smooth) average CMA trajectories for BPSK over noiseless channel $\mathbf{c}_b$.